

## Dijet production at HERA as a probe of BFKL dynamics

A.J. Askew<sup>1</sup>, D. Graudenz<sup>2</sup>, J. Kwiecinski<sup>3</sup> and A.D. Martin<sup>1</sup>

<sup>1</sup> Department of Physics, University of Durham, Durham

<sup>2</sup> Theoretical Physics Division, CERN, CH-1211 Geneva 23

<sup>3</sup> Henryk Niewodniczanski Inst. Nuclear Physics, Krakow

### Abstract

We calculate the rate for the deep-inelastic electroproduction of dijets at HERA. We study the weakening of the azimuthal (back-to-back) correlation between the jets, as  $x$  decreases, to see whether it can be used to identify BFKL dynamics from conventional fixed-order QCD effects. We show how this may give information on the transverse momentum ( $k_T$ ) dependence of the gluon distribution of the proton.

The production of dijets at the HERA electron-proton collider offers an excellent opportunity to study the properties of the gluon distribution of the proton at small  $x$ . At lowest order, dijets<sup>1</sup> are produced by the emission of a “hard” gluon from the initial or final state of the struck quark (the QCD Compton process  $\gamma q \rightarrow gq$ ) or by photon-gluon fusion ( $\gamma g \rightarrow q\bar{q}$ ). The dijet events of particular interest are those in which the two jets tend to go in the virtual photon direction (in the  $\gamma p$  centre-of-mass frame) but separated by a rapidity interval which is small relative to their large individual rapidities. In this configuration the proton-gluon fusion process dominates and small values of  $x_g$  are sampled. Here  $x_g$  is the longitudinal fraction of the proton’s momentum carried by the interacting gluon. The process is shown diagrammatically in Fig. 1, where the dominant structure of the interacting gluon at small  $x_g$  is exposed. We also show the transverse momenta  $p_{1T}$ ,  $p_{2T}$  and  $k_T$  of the outgoing (quark, antiquark) jets and the incoming gluon.

Dijets can be produced at HERA via direct photons either by photoproduction ( $Q^2 \approx 0$ ) [1, 2] or by deep-inelastic electroproduction ( $Q^2$  of  $O(10 \text{ GeV}^2)$ ). In the former case it is much more difficult to extract the direct photon events from the events in which the photon is resolved into its constituent partons [3]. In fact it appears likely that a larger “clean” dijet event sample will be obtained for electroproduction, and so we study this process. We are especially interested in the properties of the gluon at small  $x_g$ . However the values of  $x_g$  that are sampled in any deep inelastic study exposing the final state are always greater than the Bjorken  $x$ . In our case  $x_g \approx (1 + \hat{s}/Q^2)x$ , where  $\sqrt{\hat{s}}$  is the c.m. energy of the produced dijet system. So the lower the values of  $p_T$ , for which the jets can be clearly identified, the better.

In principle, the calculation of the dijet production cross section requires integration over the complete phase space of the transverse momenta  $k_T$  of the gluon. In the conventional approach we (i) restrict the integration over  $k_T^2$  to the region  $k_T^2 \ll p_{iT}^2$  and (ii) let  $k_T^2 = 0$  in the calculation of the subprocess cross section  $\hat{\sigma}(\gamma g \rightarrow q\bar{q})$ , i.e. we evaluate  $\hat{\sigma}$  with the gluon on-mass-shell. As a result we get the familiar factorization formula, which symbolically is of the form

$$x_g g(x_g, \mu^2) \otimes \hat{\sigma}(\gamma g \rightarrow q\bar{q}, \mu^2) \quad (1)$$

where the scale  $\mu^2 \sim p_{iT}^2$ . In this way we can probe the conventional gluon distribution,  $g$ , of the proton. However, at small  $x_g$ , the strong-ordering approximation is no longer applicable – we must keep the full  $k_T^2$  dependence of  $\hat{\sigma}$  and integrate over the full  $k_T^2$  phase space. As a consequence we must work in terms of the gluon distribution  $f(x_g, k_T^2, \mu^2)$  unintegrated over  $k_T^2$  [4, 5, 6], that is

$$x_g g(x_g, \mu^2) = \int^{\mu^2} \frac{dk_T^2}{k_T^2} f(x_g, k_T^2, \mu^2). \quad (2)$$

At small  $x_g$  the function  $f$  satisfies the BFKL equation [7],

$$\frac{\partial f(x_g, k_T^2)}{\partial \log(1/x_g)} = \frac{3\alpha_s}{\pi} k_T^2 \int \frac{dk_T'^2}{k_T'^2} \left[ \frac{f(x_g, k_T'^2) - f(x_g, k_T^2)}{|k_T'^2 - k_T^2|} + \frac{f(x_g, k_T^2)}{(4k_T'^4 + k_T^4)^{\frac{1}{2}}} \right], \quad (3)$$

which effectively resums the large leading  $\log(1/x_g)$  contributions which arise from the sum of the gluon emission diagrams of the type shown in Fig. 1 together with the virtual corrections. Note that, at small  $x_g$ , the gluon distribution  $f$  becomes independent of the scale  $\mu^2$ .

---

<sup>1</sup>As is customary, we use the term “dijet” to refer to two jets produced in addition to the jet formed by the remnants of the proton.

Two characteristic features of the solution of the BFKL equation are (i) the leading small  $x_g$  behaviour of the form

$$f(x_g, k_T^2) \sim x_g^{-\lambda} \quad (4)$$

where  $\lambda \approx 0.5$ , and (ii) a “diffusion” in  $k_T$  with decreasing  $x_g$  which arises from the “random-walk” in the  $k_T$  of the gluons as we proceed along the gluon chain [8, 9]. The first property gives rise to a growth in dijet production with decreasing  $x_g$ . However this behaviour can be mimicked by eq. (1) with a conventional gluon which evolves from a singular distribution at some starting scale, that is  $x_g g \sim x_g^{-\lambda}$ . The singular small  $x_g$  behaviour is stable to the evolution. The second property is more unique to BFKL dynamics. The diffusion in  $k_T$  manifests itself in a weakening of the back-to-back azimuthal correlation of the two outgoing jets of transverse momenta  $p_{1T}$  and  $p_{2T}$ . As  $x$  (and hence  $x_g$ ) decrease, larger  $k_T$ ’s are sampled and broader azimuthal distributions are expected. On the other hand the strong-ordering of the transverse momenta of conventional dijet production leads to a narrow distribution about the back-to-back jet configuration. Thus, in principle, a measurement of the azimuthal distribution offers a direct determination of the  $k_T$  dependence of the gluon distribution  $f(x_g, k_T^2)$ . In practice the situation is not so clear. The azimuthal distribution will also be broadened by higher-order conventional QCD effects. To see whether these will mask the BFKL signal we therefore also compute the azimuthal distribution resulting from the emission of a third “hard” QCD jet.

We begin by using BFKL dynamics at small  $x_g$  to calculate the differential dijet cross section as a function of  $\phi$ , the azimuthal angle between the transverse momenta  $\mathbf{p}_{1T}$  and  $\mathbf{p}_{2T}$  of the two jets. That is we evaluate

$$\frac{d\sigma}{dx dQ^2 d\phi} = \frac{4\pi\alpha^2}{Q^4 x} \left[ (1-y + \frac{y^2}{2}) \frac{dF_T(x, Q^2, \phi)}{d\phi} + (1-y) \frac{dF_L(x, Q^2, \phi)}{d\phi} \right] \quad (5)$$

where, as usual, the deep inelastic variables  $Q^2 = -q^2$ ,  $x = Q^2/2p \cdot q$  and  $y = p \cdot q / p \cdot p_e$  where  $p_e$ ,  $p$  and  $q$  are the four momenta of the incident electron, proton and virtual photon respectively, see Fig 1. The differential structure functions  $dF_i/d\phi$  can be computed from the  $k_T$ -factorization formula, which is shown symbolically in Fig. 1. It is convenient to express the jet four-momenta in terms of Sudakov variables

$$\begin{aligned} p_1 &= (1-\beta)q' + \alpha_1 p + \mathbf{p}_{1T} \\ p_2 &= \beta q' + \alpha_2 p + \mathbf{p}_{2T} \end{aligned} \quad (6)$$

where  $q' = q + xp$  and  $p$  are basic lightlike momenta. Thus, since the jets are on-mass-shell, we have

$$\alpha_1 = \left( \frac{p_{1T}^2 + m_q^2}{(1-\beta)Q^2} \right) x, \quad \alpha_2 = \left( \frac{p_{2T}^2 + m_q^2}{\beta Q^2} \right) x \quad (7)$$

where  $m_q$  is the mass of the quark. The Bjorken variable  $x \approx Q^2/2p \cdot q'$ . The factorization formula for the differential structure functions is

$$\frac{dF_i(x, Q^2, \phi)}{d\phi} = \sum_q \int_0^1 d\beta \int \frac{dp_{1T}^2 dp_{2T}^2}{k_T^4} f(x_g, k_T^2) \mathcal{F}_i^q(\beta, p_{1T}^2, p_{2T}^2, \phi) \quad (8)$$

with  $i = T, L$  and where the “factorization” variables

$$\begin{aligned} x_g &= x + \alpha_1 + \alpha_2 \quad \left( \gtrsim [1 + 4p_{iT}^2/Q^2]x \right) \\ k_T^2 &= p_{1T}^2 + p_{2T}^2 + 2p_{1T}p_{2T}\cos\phi. \end{aligned} \quad (9)$$

The functions  $\mathcal{F}_i^q$  which describe virtual photon-virtual gluon fusion,  $\gamma g \rightarrow q\bar{q}$ , at small  $x_g$  are [10]

$$\mathcal{F}_T^q(\beta, p_{1T}^2, p_{2T}^2, \phi) = e_q^2 \frac{Q^2}{8\pi^2} \alpha_s [\beta^2 + (1-\beta)^2] \left\{ \frac{p_{1T}^2 + m_q^2}{D_1^2} + \frac{p_{2T}^2 + m_q^2}{D_2^2} + 2 \frac{p_{1T} p_{2T} \cos \phi - m_q^2}{D_1 D_2} \right\} \quad (10)$$

$$\mathcal{F}_L^q(\beta, p_{1T}^2, p_{2T}^2, \phi) = e_q^2 \frac{Q^4}{2\pi^2} \alpha_s \beta^2 (1-\beta)^2 \left\{ \frac{1}{D_1^2} + \frac{1}{D_2^2} - \frac{2}{D_1 D_2} \right\} \quad (11)$$

where  $e_q$  is the charge of the quark  $q$  and where the denominators

$$D_i = p_{iT}^2 + m_q^2 + \beta(1-\beta)Q^2. \quad (12)$$

The first two terms in  $\{\dots\}$  in (10) and (11) correspond to quark box contributions with  $p_1$  being first a quark and then an antiquark jet, whereas the third term is the “crossed-box” interference term. Note that the apparent divergence of the integral in (8) at  $k_T^2 = 0$  (that is at  $\phi = \pi$ ) is cancelled by the zeros of the functions  $f$  and  $\mathcal{F}_{T,L}$ , see (10) and (11).

The only unknown in the determination of the differential cross section for deep-inelastic dijet production,  $d\sigma/dxdQ^2d\phi$ , is the gluon distribution  $f(x_g, k_T^2)$  that enters in (8). We calculate  $f$  by solving the differential form of the BFKL equation, (3), using knowledge of the gluon at  $x_g = 10^{-2}$ , as described in ref.[9]. The normalisation (though not the  $x_g$  behaviour) of  $f$  is dependent on the treatment of the infrared  $k_T$  region. However, the gluon distribution  $f$  can also be used to predict the behaviour of the structure function  $F_2$  itself, via the inclusive form of the  $k_T$ -factorization formula (8), see ref.[9]. Thus we can fix the infrared parameter in the determination of  $f$  so as to reproduce the low  $x$  measurements of  $F_2$  at HERA[12]. The result is shown by continuous curves in Fig.2, and corresponds to the choice  $k_a^2 = 2 \text{ GeV}^2$ . We see that an excellent description of  $F_2$  is obtained. Now that  $f$  has been fully specified in this way, we should be able to predict the azimuthal distribution reliably, provided, of course, that we sample sufficiently small values of  $x_g$  for the BFKL solution to be appropriate.

In Fig. 3(a) we show  $dF_T/d\phi$  calculated from the  $k_T$ -factorization formula, (8), for deep-inelastic dijet events with  $Q^2 = 10 \text{ GeV}^2$  for three different values of  $x$ . Each jet is required to have transverse energy squared,  $E_T^2$ , greater than  $10 \text{ GeV}^2$ . We notice a rapid increase in the dijet rate with decreasing  $x$ , and a weakening of the azimuthal back-to-back correlation. This last observation is more evident from Fig. 3(b) which shows the same distributions normalized to a common maximum value at  $\phi = \pi$ . The broadening with decreasing  $x$  is a manifestation of the diffusion in  $k_T$  which is characteristic of BFKL dynamics. The detailed shape in the region of  $\phi \approx \pi$  may not be reliable, since it corresponds to small values of the transverse momentum  $k_T$ , of the gluon (see Fig. 1). Moreover hadronization effects will influence the distribution in this region. Rather we should study the normalised distribution,  $dF_T/d\phi$ , away from  $\phi = \pi$ , say outside the interval  $180 \pm 20$  degrees.

The characteristic BFKL behaviour of the solution  $f(x, k_T^2)$  of (3) only has a chance to set in for  $x \lesssim 10^{-3}$ . The precocious onset of this leading  $\log(1/x)$  behaviour does indeed appear compatible with the striking rise of  $F_2$  with decreasing  $x$  that has been observed at HERA, see Fig.2. However this is not conclusive evidence of BFKL dynamics. The  $F_2$  data can equally well be described by Altarelli-Parisi (or GLAP) evolution. For example the dashed curves in Fig.2 are the description obtained from a recent global structure function analysis based on (next-to-leading order) GLAP evolution from “singular” parton distributions at  $Q^2 = 4 \text{ GeV}^2$ [13]. To

distinguish BFKL dynamics from conventional QCD we must look into properties of the final state at small  $x$ , such as the weakening of the back-to-back correlations in the dijet events. However there is a price to pay. The BFKL dynamics is sampled at larger “ $x$ ” for final state processes than is the case for the inclusive  $F_2$  measurement. In our example of dijets with  $E_T^2(\text{jet}) > 10 \text{ GeV}^2$  and  $Q^2 = 10 \text{ GeV}^2$ , we see from (9) that we sample values of  $x_g \gtrsim 5x$ . Thus if  $f(x_g, k_T^2)$  assumes a characteristic BFKL behaviour for  $x_g \lesssim 10^{-3}$ , then we anticipate that the broadening of the  $\phi$  distribution, with decreasing  $x$ , will only be relevant in the region  $x \lesssim \text{few} \times 10^{-4}$ . This is near the limit of the region which is at present accessible at HERA. In Fig.4 we therefore compare the dijet azimuthal distribution for  $x = 2 \times 10^{-4}$  with that for  $x = 10^{-3}$ , that is two values of  $x$  which are appropriate for HERA.

As mentioned above, the weakening of the back-to-back azimuthal correlations can also be obtained in a more conventional way from fixed-order QCD effects, in particular from 3+1 jet production. As usual the +1 refers to the jet associated with the remnants of the proton. Part of the 3+1 jet production is, of course, already included in the calculation based on BFKL dynamics, since the absence of strong-ordering in  $k_T$  means that the gluonic ladder contains additional (gluon) jets. Before drawing final conclusions we must therefore compare our BFKL dijet predictions with the azimuthal distribution coming from conventional 3+1 jet production. To calculate the latter we use the PROJET Monte Carlo [14]. We require two of the jets to have  $E_T^2(\text{jet } 1, 2) > 10 \text{ GeV}^2$  and the third to have  $E_T^2(\text{jet } 3) < 10 \text{ GeV}^2$ , chosen so that two jets are “visible” and the third (which may be either a gluon or a quark) is relatively “soft”. The results are shown by the histograms superimposed on Fig.4. We have checked that the PROJET predictions in the region  $|\phi - \pi| \gtrsim 20^\circ$  are not sensitive to a reasonable variation of the cut-off,  $y_{ij} \equiv s_{ij}/W^2 > y_0$ , that is used to regulate the infrared singularities.

We see from Fig.4 that the appearance of dijet events in the “tails” of the azimuthal distribution, that is at angles such that  $|\phi - \pi| \gtrsim 45^\circ$ , at the predicted rate, will be a distinctive signal for BFKL dynamics. Nearer the back-to-back configuration the fixed-order QCD processes swamp the BFKL effect. Of course, since we work at the parton level and ignore the experimental problems of jet identification, only the BFKL signal can contribute for  $|\phi - \pi| > 60^\circ$ . If the cut,  $E_T^2(\text{jet } 3) < 10 \text{ GeV}^2$ , on the third jet is removed and the azimuthal distribution is plotted as a function of the angle,  $\phi$ , between the two jets with the largest  $E_T$ ’s then the PROJET prediction is essentially unchanged for  $|\phi - \pi| \approx 20^\circ$ , but is enhanced at larger angles with a steeper fall off towards the limiting angle  $|\phi - \pi| = 60^\circ$ .

The deep inelastic variables ( $x, Q^2$ ) and jet cuts ( $E_T > E_{0T}$ ) have been chosen in an attempt to optimize both the event rate and the BFKL signal at HERA. Clearly if we were able to go to smaller  $x$  (or, to be precise, smaller  $x_g$ ) then the BFKL effect would be more pronounced, see Fig.3. Now the observable deep inelastic region at HERA lies in the domain  $Q^2/x \lesssim 10^5 \text{ GeV}^2$ . On the other hand, we see from (9) that  $x_g \gtrsim x + 4(x/Q^2)E_{0T}^2$ , when two jets with  $E_T > E_{0T}$  are recorded. A higher jet threshold,  $E_{0T}$ , has the advantage that the fixed-order QCD contribution is suppressed relative to the BFKL signal, but (since  $Q^2/x$  is bounded) then a higher  $x_g$  is sampled. The lower plot in Fig.4 shows the results for  $Q^2 = E_{0T}^2 = 25 \text{ GeV}^2$  and  $x = 5 \times 10^{-4}$ , for which  $x_g$  is increased by a factor of 2.5 in comparison to that sampled for  $Q^2 = E_{0T}^2 = 10 \text{ GeV}^2$  and  $x = 2 \times 10^{-4}$ .

To sum up, the main aim of our paper is to quantify the observation that BFKL dynamics weakens the azimuthal correlation of the  $q, \bar{q}$  jets produced in small  $x$  deep-inelastic scattering via the photon-gluon fusion mechanism. We are able to obtain an absolute prediction since

the parameter which specifies the infrared contribution to the BFKL equation is chosen such that the measurements of  $F_2$  at HERA are reproduced. (That a physically reasonable choice of a single infrared parameter suffices to describe the observed small  $x$  behaviour of  $F_2$  is a far from trivial test of BFKL dynamics.) For the dijet events we find a substantial broadening of the azimuthal distribution and an increase of this broadening with decreasing  $x$ . However, at HERA energies, we find that the fixed-order QCD contribution from 3+1 jet production exceeds the BFKL signal near the back-to-back configuration. Nevertheless at sufficiently large values of  $|\phi - \pi|$  BFKL dynamics dominates and give rise to a distinctive “tail” to the azimuthal distribution at an observable rate. In this way dijet production at HERA offers an opportunity to study the  $k_T$  dependence of the gluon distribution of the proton.

## Acknowledgements

We thank Nigel Glover, Genya Levin, Al Mueller, Albert De Roeck and Peter Sutton for valuable discussions. This work has been supported in part by the Polish KBN grant 2 P302 062 04, by the UK PPA Resesarch Council and the EU under contract no. CHRX-CT92-0004. One of us (AJA) thanks the Polish KBN - British Council collaborative research programme for support.

## References

- [1] A. Derrick et al., Phys. Lett. **B322** (1994) 287
- [2] J.R. Forshaw and R.G. Roberts, RAL preprint 94-028, March 1994
- [3] A. De Roeck, private communication
- [4] S. Catani, F. Fiorani and G. Marchesini, Phys. Lett. **B234** (1990) 339; Nucl. Phys. **B336** (1990) 18
- [5] S. Catani, M. Ciafaloni and F. Hautmann, Phys. Lett. **B242** (1990) 190; Nucl. Phys. **B366** (1991) 135
- [6] J.C. Collins and R.K. Ellis, Nucl. Phys. **B360** (1991) 3
- [7] E.A. Kuraev, L.N. Lipatov and V. Fadin, Phys. Lett. **60B** (1975) 50, Zh. Eksp. Teor. Fiz. **72** (1977) 373 [Sov. Phys. JETP **45** (1977) 199]; Ya.Ya. Balitskij and L.N. Lipatov, Yad. Fiz. **28** (1978) 1597 [Sov. J. Nucl. Phys. **28** (1978) 822]; L.N. Lipatov, in “Perturbative QCD”, edited by A.H. Mueller, World Scientific, Singapore, 1989, p. 411; J.B. Bronzan and R.L. Sugar, Phys. Rev. **D17** (1978) 585; T. Jaroszewicz, Acta Polon. **B11** (1980) 965
- [8] J. Bartels and A. Lotter, Phys. Letts. **B309** (1993) 400
- [9] A.J. Askew, J. Kwiecinski, A.D. Martin and P.J. Sutton, Phys. Rev. **D49** (1994) 4402
- [10] A.J. Askew, J. Kwiecinski, A.D. Martin and P.J. Sutton, Phys. Rev. **D47** (1993) 3775
- [11] M. Ciafaloni, Nucl. Phys. **B296** (1988) 49
- [12] H1 collaboration: I. Abt et al., Nucl. Phys. **B407** (1993) 515; K. Müller, Proc. of 29th Rencontre de Moriond, March 1994  
ZEUS collaboration: M. Derrick et al., Phys. Lett. **B316** (1993) 412; G. Wolf, Proc. of International Workshop on Deep Inelastic Scattering, Eilat, Israel, Feb. 1994; M. Roco, Proc. of 29th Rencontre de Moriond, March 1994
- [13] A.D. Martin, W.J. Stirling and R.G. Roberts, Durham preprint DTP/94/34, June 1994
- [14] D. Graudenz, PROJET: Jet cross sections in deep inelastic electron-proton scattering, version 3.6, to be published.

## Figure Captions

- Fig. 1 A diagrammatic representation of dijet production by photon-gluon fusion,  $\gamma g \rightarrow q\bar{q}$ , at small  $x_g$ . The function  $f$  is the (unintegrated) gluon distribution of the proton. The cross section is given by the  $k_T$ -factorization formula (8), which has the symbolic form  $\sigma = f \otimes \mathcal{F}$ .  $\mathcal{F}$  denotes the quark box (and crossed box) contribution.
- Fig. 2 The measurements of  $F_2$  at HERA (preliminary data from the 1993 run[12]) shown together with the BFKL description[9] (continuous curves) and the MRS(A) parton analysis fit[13] (dashed curves). The measurements of the H1 collaboration at  $Q^2 = 65 \text{ GeV}^2$  are shown on the  $Q^2 = 60 \text{ GeV}^2$  plot.
- Fig. 3 (a) The distribution  $dF_T/d\phi$  predicted by the BFKL  $k_T$ -factorization formula, (8), for deep-inelastic dijet events with  $Q^2 = 10 \text{ GeV}^2$  and  $E_T^2(\text{jet}) > 10 \text{ GeV}^2$ . (b) The distributions normalized to a common maximum.
- Fig. 4 The curves are the differential cross section for dijet production predicted by BFKL dynamics, (5)-(12), whereas the histograms correspond to 3+1 jet production as determined by the PROJET Monte Carlo using MRS(A) partons [13]. In the first case, the broadening of the azimuthal distribution arises from the  $k_T$  dependence of the gluon distribution  $f(x_g, k_T^2)$  found by solving the BFKL equation, (3). For 3+1 jet production we assume that the third jet has  $E_T^2 < 10(25) \text{ GeV}^2$  in the upper (lower) plot.



This figure "fig1-1.png" is available in "png" format from:

<http://arXiv.org/ps/hep-ph/9407337v1>

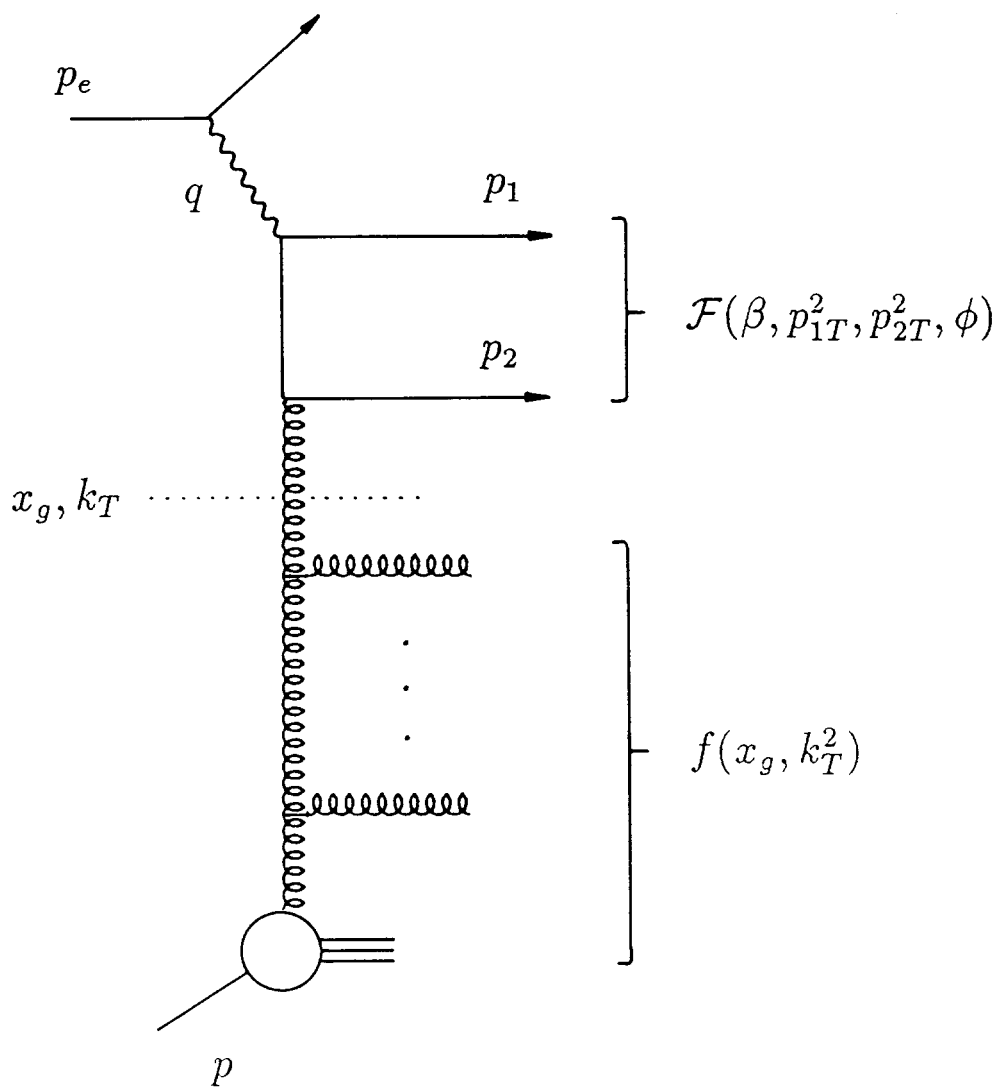


*Fig. 1*

This figure "fig1-2.png" is available in "png" format from:

<http://arXiv.org/ps/hep-ph/9407337v1>

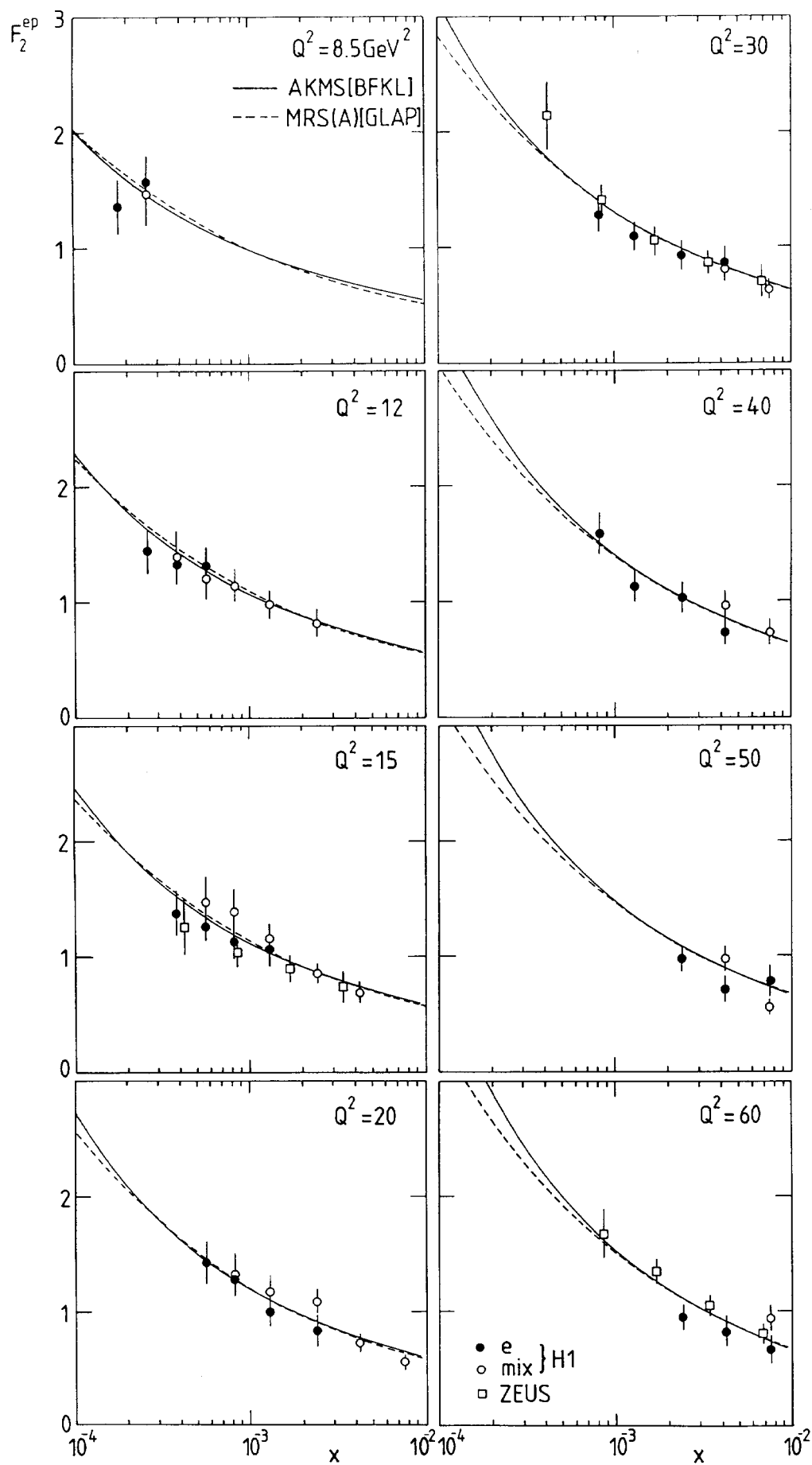


Fig. 2

This figure "fig1-3.png" is available in "png" format from:

<http://arXiv.org/ps/hep-ph/9407337v1>

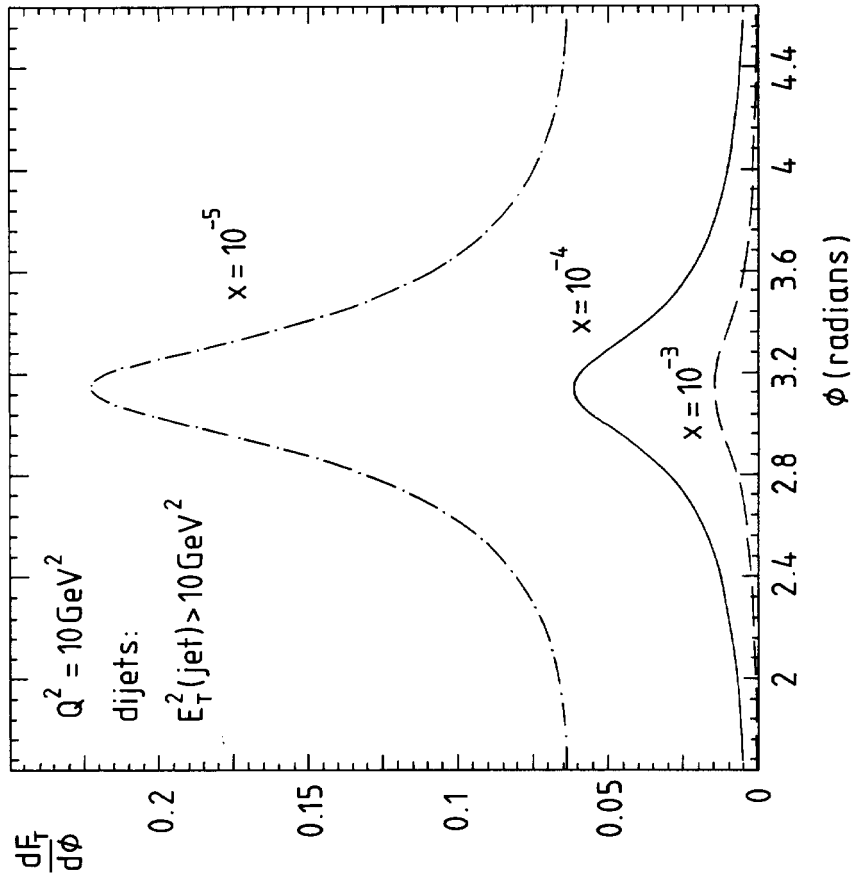


Fig.3(a)

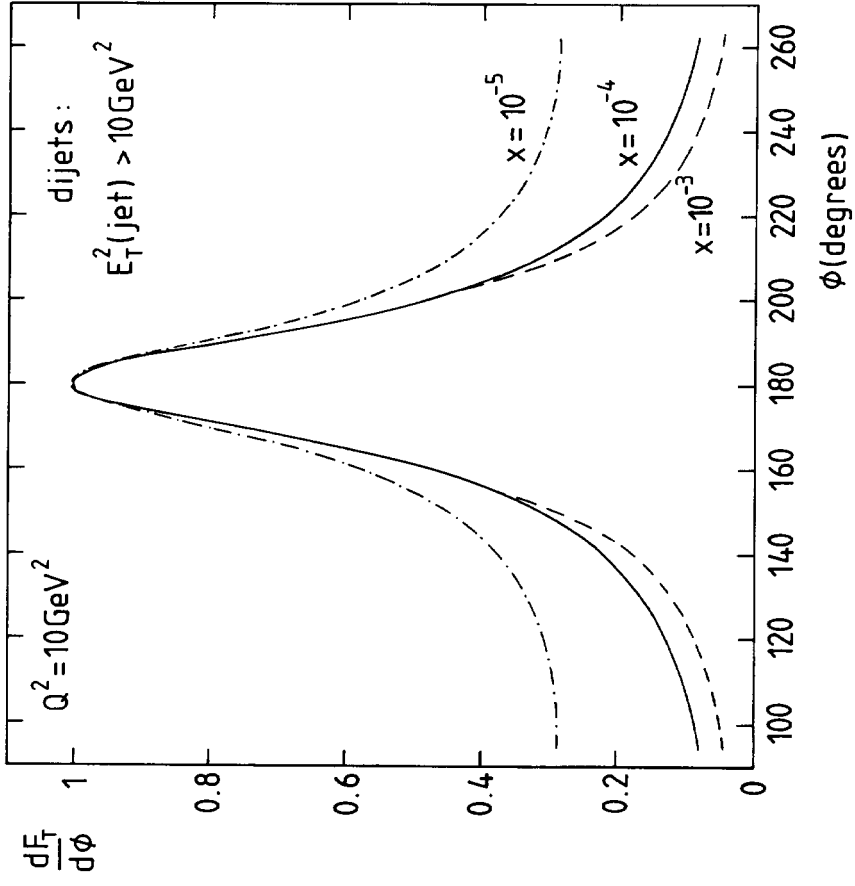


Fig.3(b)

This figure "fig1-4.png" is available in "png" format from:

<http://arXiv.org/ps/hep-ph/9407337v1>

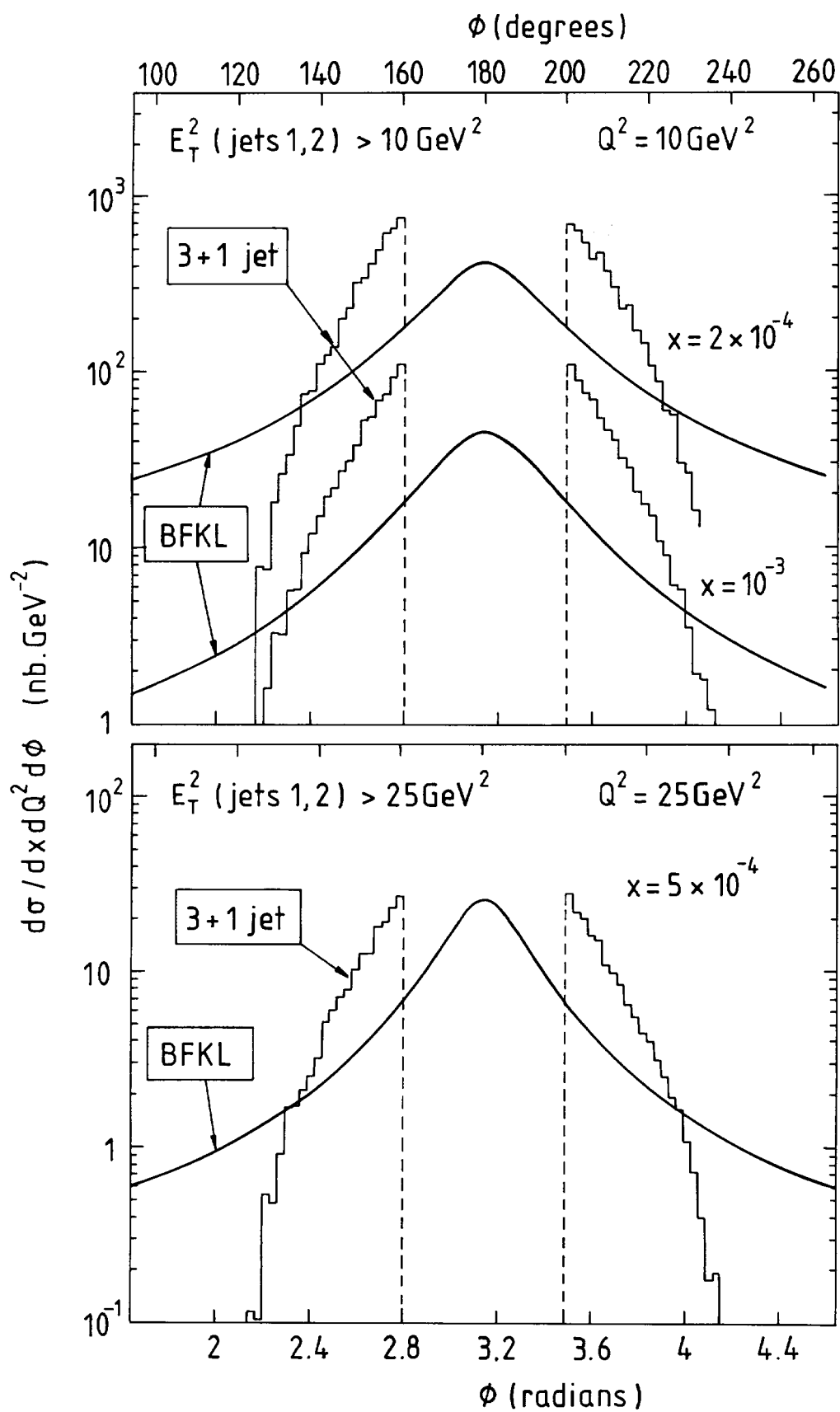


Fig. 4